Microwave properties and characterization of co-evaporated BSCCO thin films

F A Miranda†, C M Chorey‡, M A Stan§, C E Nordgren‖, R Y Kwor¶ and T S Kalkur¶

† National Aeronautics and Space Administration, Lewis Research Center, Cleveland, OH 44135
‡ Sverdrup Technology, Inc. Lewis Research Center Group, Brook Park, OH 44142
§ Department of Physics, Kent State University, Kent, OH 44242
‖ Department of Physics, Case Western Reserve University, Cleveland, OH 44106
¶ Department of Electrical and Computer Engineering, University of Colorado at Colorado Springs, Colorado Springs, CO 80933, USA

Received 25 February 1992, in final form 21 April 1992

Abstract. An extensive characterization of Bi–Sr–Ca–Cu–O (BSCCO) thin films deposited by co-evaporation on $LaAlO_3$ and $SrTiO_3$ substrates has been performed. The films had a $T_c(R = 0)$ of ~78 K, and were predominantly *c*-axis oriented, with critical current densities (J_c) at 4.5 K of 1.6×10^6 and 1.1×10^6 A cm^{-2}, for the samples on $SrTiO_3$ and $LaAlO_3$ respectively. The microwave properties of the films were examined by three techniques. The complex conductivity ($\sigma^* = \sigma_1 - j\sigma_2$) and the magnetic penetration depth (λ) were measured by power transmission at 30.6 GHz; the surface resistance (R_s) was measured using a cavity resonator at 58.9 GHz, and the transmission line losses were determined by measuring the quality factor (Q) of a linear microstrip resonator at 10.4 and 20.2 GHz. The complex conductivity for the film on $LaAlO_3$ was determined to be $(2.0 - j10) \times 10^5$ S m^{-1} at 77 K. It was observed that in the superconducting state σ_1 deviates from both the Bardeen–Cooper–Schrieffer (BCS) theory and the two-fluid model. Values of λ were found to be ~2.0 and 1.1 μm at 77 K and 20 K respectively, and were obtained for the film on $LaAlO_3$. The value of λ at 20 K was approximately three times larger than that of BSCCO single crystals. R_s values of 865 and 1391 mΩ were obtained for the films on $SrTiO_3$ and $LaAlO_3$, respectively, at 77 K and 58.9 GHz. Unloaded Q factors at 20 K of ~1100 and 800 at 10.4 and 20.2 GHz respectively, were measured for the BSCCO resonator. Unloaded Q values of 290 and 405 at 20 K were obtained at 10.4 GHz and 20.2 GHz respectively, for an all gold (Au) resonator.

1. Introduction

High transition temperature superconductors (HTS) have potential for microwave applications due to their low loss and dispersion as compared with typically used conductors such as copper (Cu) and gold (Au). Therefore, it is not surprising that to date a large number of measurements at microwave frequencies on HTS properties such as surface resistance (R_s), complex conductivity ($\sigma^* = \sigma_1 - j\sigma_2$), and magnetic penetration depth (λ), have been reported. Most of the work so far has been performed on the $YBa_2Cu_3O_{7-\delta}$ (YBCO) compound [1–7], mainly because of its single phase and simplicity of fabrication. However, studies of the Bi–Sr–Ca–Cu–O (BSCCO) compound have been performed by several research groups since this material offers the advantage of being relatively insensitive to exposure to atmosphere and handling, and because of its great stability with respect to thermal cycling [8]. In spite of the number of studies on BSCCO thin films, data on R_s and σ^* at microwave frequencies are still scarce [9, 10].

In this paper we report on the structural, DC and microwave properties of two BSCCO thin films deposited by co-evaporation on $LaAlO_3$ and $SrTiO_3$ substrates. The films were characterized by scanning electron microscopy (SEM), x-ray diffraction (XRD) analysis, by DC transition temperature (T_c) and critical current density (J_c) measurements. The microwave properties of the films were determined from R_s measurements using resonant cavity techniques, and power transmission measurements. The R_s of the film on $LaAlO_3$ was also measured using a linear resonator

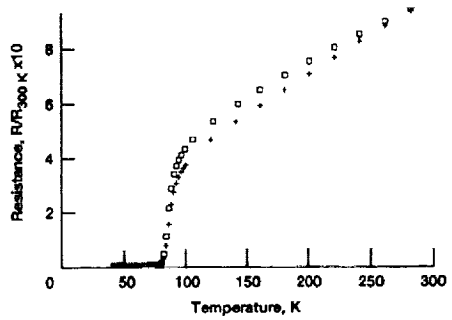

Figure 1. Normalized resistance against temperature for BSCCO thin films (3000 Å) on $SrTiO_3$ (+ : $T_c(R = 0) = 78.2$ K) and $LaAlO_3$ (□: $T_c(R = 0) = 78$ K) substrates.

method, since knowledge of the microwave signal propagation along transmission lines is of interest for practical microwave applications.

2. Structure and DC properties

Our measurements were made on BSCCO superconducting films approximately 3000 Å thick deposited by co-evaporation on to (100) $LaAlO_3$ and (100) $SrTiO_3$ substrates 0.010 in thick. The details of the BSCCO film preparation can be found elsewhere [11]. The $T_c(R = 0)$ of the films was determined using standard four-point-probe measurement techniques. T_c values of 78.2 and 78.0 K were measured for the films on $SrTiO_3$ and $LaAlO_3$ respectively (figure 1). Both films have a transition width (ΔT) of ~ 10 K, which is consistent with previously reported resistivity data for BSCCO thin films [12]. The zero temperature intercept (R_o) is lower for the film on $SrTiO_3$, and suggests a higher degree of c-axis texturing, where the c axis is perpendicular to the substrate plane.

Figure 2 shows SEM micrographs of the films under study. The observed surface roughness is typical of films grown by high temperature *ex-situ* anneal. However, surface roughness alone has not been shown to be detrimental to microwave properties of HTS thin films [7, 13]. Note that the background structure shows the plate-like structure typical of the BSCCO system. The typical grain size for these films was between 2 and 10 μm. XRD analysis of these films showed that they were predominantly oriented with the c axis perpendicular to the film plane, although unknown peaks were observed in both samples, as shown in figure 3. The c-axis lattice parameter agrees within 1 per cent of that corresponding to single crystals [14].

Magnetization hysteresis measurements were performed using a Quantum Design Magnetic Property Measurement System (MPMS). For these measurements, rectangular samples were cut from the films on $SrTiO_3$ and $LaAlO_3$, and the samples were oriented with the a–b plane normal to the magnetic field (H). Figure 4 shows magnetization hysteresis loops for both films.

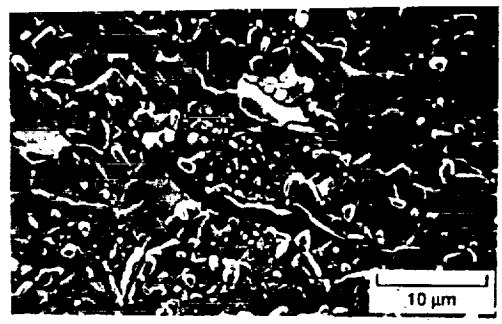

(a)

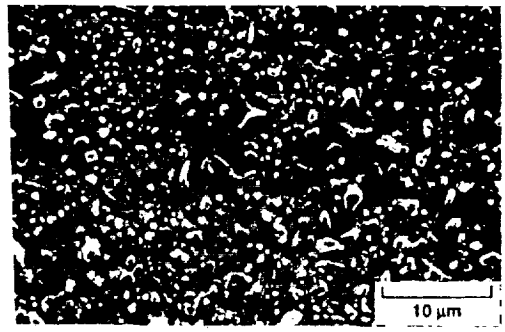

(b)

Figure 2. Scanning electron micrographs of the surface of co-evaporated (3000 Å) BSCCO thin films on (*a*) $SrTiO_3$, and (*b*) $LaAlO_3$.

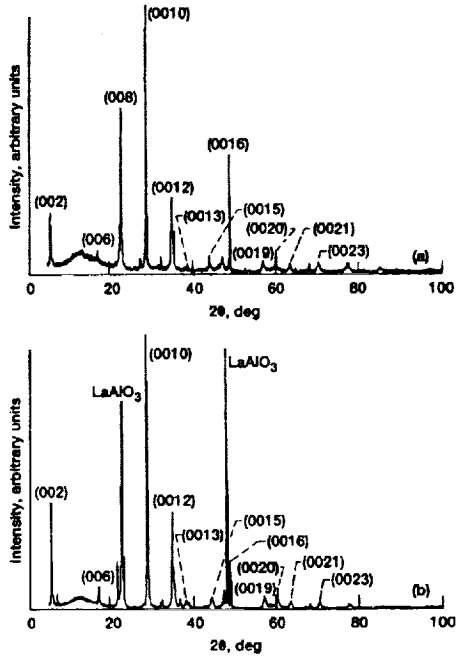

Figure 3. X-ray diffraction pattern of 3000 Å BSCCO HTS thin films on (*a*) $SrTiO_3$, and (*b*) $LaAlO_3$ substrates. The films are predominantly the $Bi_2Sr_2Ca_1Cu_2O_x$ (2212) phase with the c axis perpendicular to the substrate.

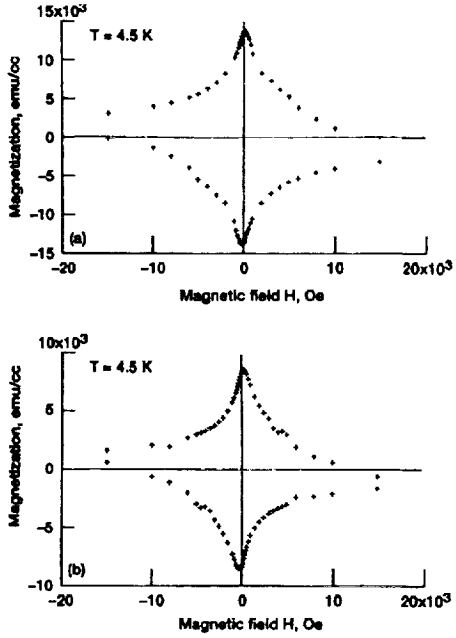

Figure 4. Magnetization hysteresis loops for BSCCO thin films (3000 Å) on (*a*) $SrTiO_3$, and (*b*) $LaAlO_3$; H parallel to the c axis.

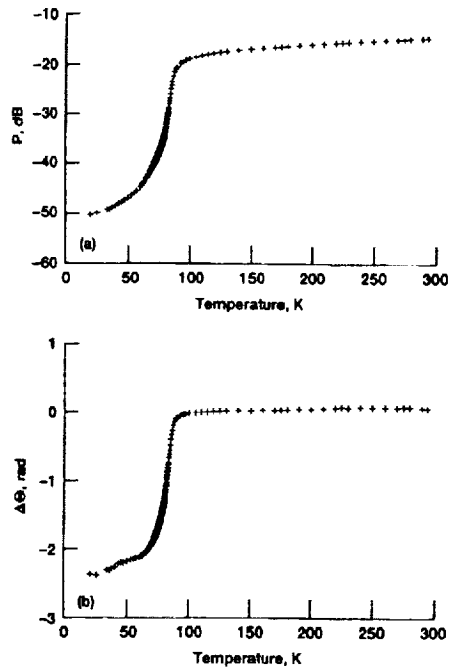

Figure 5. Magnitude, P, (*a*) and relative phase, $\Delta\theta = \theta_{300\,K} - \theta(T)$ (*b*) of the fractional transmitted power for a co-evaporated BSCCO thin film (3000 Å) on $LaAlO_3$ at 30.6 GHz.

Using Bean's model [15], and assuming a circular current path, we obtained J_c values at 4.5 K of 1.6×10^6 and 1.1×10^6 A cm^{-2} for the films on $SrTiO_3$ and $LaAlO_3$ respectively. J_c values for both films are listed in table 1 as a function of temperature. Note that for all temperatures the J_c obtained for the film on $SrTiO_3$ is larger than that for the film on $LaAlO_3$, which may be a result of better epitaxy on the $SrTiO_3$ substrate. In addition, the J_c values for both films at 40 K agree well with the $J_c \sim 1.5 \times 10^5$ A cm^{-2} reported at 40 K for laser-ablated BSCCO thin films (~3000 Å) on MgO [12].

3. Characterization of BSCCO films at microwave frequencies

3.1. Power transmission measurements

Power transmission measurements were performed on the samples at frequencies from 26.5 to 40.0 GHz (Ka-band), and at temperatures from 300 to 20 K. The details of the experimental configuration and measurement procedures have been previously reported [7]. The main components of the experimental apparatus are an HP-8510B network analyser and a closed-cycle helium gas refrigerator, both controlled by an HP 900-216 computer. The network analyser is coupled to the refrigerator by Ka-band rectangular waveguides. The measurement technique compares the transmitted signal with the incident microwave signal to determine the power transmission coefficient. All the measurements were made under vacuum ($<10^{-3}$ Torr) in a vacuum can with input/output ports for the waveguides designed for the refrigerator. Inside the vacuum can the sample was oriented perpendicular to the microwave source by clamping it between two waveguide flanges thermally connected to the cold head of the refrigerator through a gold-plated copper plate. The film side of the sample was directed towards the incident microwave signal. The system was calibrated before the beginning of each measurement cycle to account for the impedance and spurious reflections of the waveguide network. Background attenuation and phase corrections were made by subtracting the transmitted power as a function of temperature in the absence of the sample from the data obtained with the sample in place.

Figure 5 shows a plot of the magnitude (P) and relative phase ($\Delta\theta$, where $\Delta\theta = \theta_{RT} - \theta(T)$, with θ_{RT} the phase value at room temperature) at 30.6 GHz of the fractional transmitted power for the film on the $LaAlO_3$

Table 1. Magnetic J_c for BSCCO thin films on $SrTiO_3$ and $LaAlO_3$ substrates.

Temperature (K)	J_c (A cm^{-2})	
	$SrTiO_3$	$LaAlO_3$
4.5	1.6×10^6	1.1×10^6
20.0	1.0×10^6	6.7×10^5
40.0	2.7×10^5	1.0×10^5

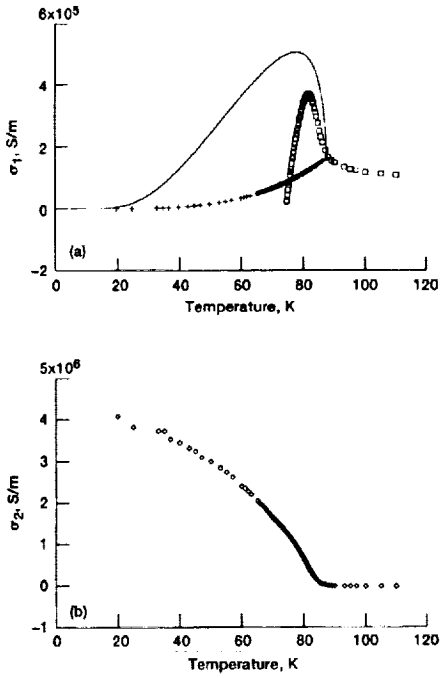

Figure 6. Real (*a*) and imaginary (*b*) parts of the complex conductivity against temperature at 30.6 GHz for a co-evaporated BSCCO thin film (3000 Å) on $LaAlO_3$. In (*a*) □ represents the experimental data, + represents σ_1 obtained using the two-fluid model approximation, and the solid line represents a fit using the BCS temperature dependence for σ_1.

substrate as a function of temperature. Since in this type of measurement the signal also interacts with the substrate, similar types of measurement were not performed with the film on $SrTiO_3$ because of the extreme temperature sensitivity of its dielectric constant and loss tangent [16, 17]. $LaAlO_3$ has more stable properties and has proved to be a suitable substrate for microwave applications [18, 19]. Observe that in the normal state P decreases monotonically with temperature while $\Delta\theta$ remains almost constant. However, at the beginning of the normal-superconducting phase transition (~88 K) both P and $\Delta\theta$ decrease very quickly, levelling off at low temperatures. This behaviour is consistent with previous reports for BSCCO and YBCO thin films [7, 20, 21].

The complex conductivity can be expressed in terms of the power transmission data according to the following relations [7],

where R and I are the real and imaginary parts of the HTS thin film dispersion coefficient and are related to σ^* by $R = 1 + 4\pi\sigma_2/\omega\varepsilon$, and $I = 4\pi\sigma_1/\omega\varepsilon$, where $\omega/2\pi = f$ is the frequency of the wave and ε is the relative dielectric constant of the HTS material. P and θ were measured, and from these quantities σ^* was calculated.

Figure 6 shows plots of σ_1 and σ_2 against temperature for the BSCCO film on $LaAlO_3$. Observe that in the normal state σ_1 shows metallic behaviour, while σ_2 is close to zero as expected for a good conductor. When the superconducting transition begins (we refer to this temperature as T_c^{mw}, which in this case is ~88 K), both conductivities increase rapidly. As the temperature decreases, σ_1 increases to a maximum and then decreases quickly to the extent that we were unable to determine its value for temperatures below ~74 K, while σ_2 increased monotonically. This behaviour is consistent with that reported for YBCO and other BSCCO thin films [7, 20, 21]. The complex conductivity was determined to be $(2.0 - j10) \times 10^5$ S m^{-1} at 77 K. These values are approximately one order of magnitude larger than those obtained previously for BSCCO thin films on $LaAlO_3$ at the same temperature and frequency [10]. The same temperature behaviour for σ^* was observed for measurements at other frequencies within the Ka-band. From figure 6(*a*) it can be seen that the behaviour of σ_1 in the superconducting state does not follow that expected from the two-fluid model approximation [22] where,

$$\sigma_1(T) = \sigma_c(T/T_c)^4 \tag{3}$$

and σ_c is the conductivity at T_c. The measured data also deviated from σ_1 calculated using the BCS-based Mattis–Bardeen equations [23]

$$\sigma_1 = \sigma_c[2\Delta(k_B T)^{-1}] \exp[-\Delta/k_B T] \ln(\Delta/\hbar\omega) \quad \hbar\omega \ll 2\Delta \tag{4}$$

where k_B is Boltzmann's constant, $\omega = 2\pi f$ is the angular frequency, and Δ is the energy gap.

The values of σ_2 can be used to determine λ by using the expression $\lambda = (1/\mu\omega\sigma_2)^{1/2}$, valid for homogeneous superconductors. λ values of ~1.97 and 1.09 μm at 77 and 20 K respectively, were obtained for the film on $LaAlO_3$. The value of λ at low temperature is less than that obtained in ion-beam-deposited BSCCO thin films on MgO ($\lambda \sim 1.3$ μm) [20], and compare well with those obtained using microstrip transmission lines fabricated with the same type of co-evaporated BSCCO films used in this study ($\lambda(0) \sim 1.11$ μm, where $\lambda(0)$ is the magnetic penetration depth at

$$R = \frac{\{(2n/P^{1/2})[n\cos(k_0 nt)\sin(k_0 t + \theta) - \sin(k_0 nt)\cos(k_0 t + \theta)] - n(n^2 - 1)\sin(k_0 nt)\cos(k_0 nt)\}}{k_0 d[n^2\cos^2(k_0 nt) + \sin^2(k_0 nt)]} \tag{1}$$

and

$$I = \frac{\{(2n/P^{1/2})[n\cos(k_0 nt)\cos(k_0 t + \theta) + \sin(k_0 nt)\sin(k_0 t + \theta)] - 2n^2\cos^2(k_0 nt) - (n^2 + 1)\sin^2(k_0 nt)\}}{k_0 d[n^2\cos^2(k_0 nt) + \sin^2(k_0 nt)]} \tag{2}$$

$T = 0$) [24]. However, the values of λ are still large when compared with those reported for BSCCO single-crystals ($\lambda(0) \sim 0.3$ μm) [25–27].

3.2. Surface resistance measurements

Cavity method The R_s of the films was measured by monitoring the change in the quality factor (Q) of a cylindrical, TE_{011} mode copper cavity, resonant at 58.9 GHz, with one of its end walls replaced with the BSCCO thin film. Using an HP-8510B network analyser and Ginzton's impedance method the loaded Q (Q_L) of the cavity was determined by measuring the reflection coefficient. Knowing Q_L, the unloaded quality factor (Q_o) of the cavity was obtained and the R_s of the BSCCO films were computed by the method in [28]. As shown in Figure 7, the R_s of the BSCCO films decreased monotonically with temperature for $T/T_c > 0.75$, levelling off at lower temperatures. Note that, except for very low temperatures, the R_s for the film on $SrTiO_3$ is less than that of its counterpart on $LaAlO_3$. Values of R_s of 865 and 376 mΩ for the film on $SrTiO_3$, and of 1391 and 370 mΩ for the film on $LaAlO_3$ were obtained at 77 and 20 K respectively. The R_s values at low temperatures are almost one-fifth of those measured at lower frequencies on BSCCO films on MgO using microstrip and cavity resonator techniques ($\sim$25 mΩ at 7 GHz and 25 K; $R_s \sim 1770$ mΩ at 58.9 GHz assuming $R_s \propto f^2$ dependence) [29]. They are also almost an order of magnitude less than those recently obtained by others from ring microstrip resonators fabricated on e-beam deposited BSCCO films on MgO ($\sim$34 mΩ at 4.2 K, 6 GHz, and 12 dB m incident RF power; 3276 mΩ at 4.2 K, 58.9 GHz, using $R_s \propto f^2$) [30]. Since the R_s of the film is larger than that of Cu for all temperatures (for very pure Cu and at 77 K, $R_s \sim 21.6$ mΩ at 58.9 GHz; the measured R_s value for a Cu sample at 77 K using the cavity was $\sim$45.4 mΩ) the flat part of the curve may be associated with residual losses in the film and not with limitations in the sensitivity of the cavity, in contrast to measurements of good quality YBCO thin films on $LaAlO_3$ [7].

Linear resonator method Microstrip transmission line resonators were fabricated and tested to examine the losses of the BSCCO films in a structure that can be used in potential HTS passive microwave circuits such as filters, resonators or delay lines. The microstrip structure is shown in figure 8 and consisted of the BSCCO superconducting strip separated from a gold ground plane by the 0.010 in $LaAlO_3$ substrate (figure 8(*a*)). The strip width (W) was 300 μm with a length (L) of 7 mm (figure 8(*b*)). This resulted in a 30 Ω line impedance with the fundamental ($L = \lambda/2$) resonant frequency at 10.4 GHz and a second harmonic ($L = \lambda$) at 20.2 GHz. The resonant strip was capacitively coupled to a 30 Ω feed line by a 75 μm wide gap (G). Transition from the coaxial test cables to the microstrip feed line was accomplished by a coaxial 'spark-plug' launcher.

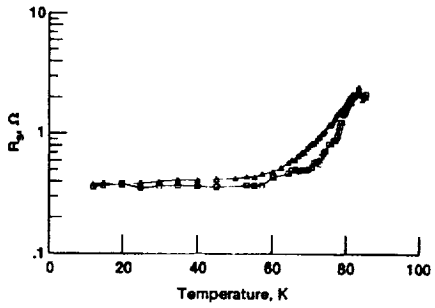

Figure 7. Surface resistance, R_s, at 58.9 GHz against temperature for co-evaporated BSCCO thin films (3000 Å) on $SrTiO_3$ (□) and $LaAlO_3$ (△).

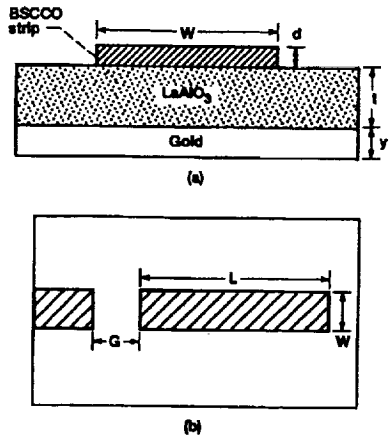

Figure 8. Cross section (*a*), and top view (*b*) of a BSCCO microstrip transmission line resonator. For this resonator $W = 300$ μm, $L = 7$ mm, $G = 75$ μm, $d = 3000$ Å, $t = 0.010$ in, and $y = 1.5$ μm. The calculated line impedance was 30 Ω.

The circuit was tested using an HP 8510B network analyser and a closed-cycle refrigerator for cooling. The test cable was calibrated up to the spark-plug launcher using coaxial open, short, and load standards. The calibration was performed at room temperature but was used at low temperatures as well since only minor shifts in the calibration with decreasing temperature were observed. The reflection coefficient (S_{11}) was measured at temperatures from $\sim$20 K upwards, giving the loaded Q of the circuit. Using the impedance method [31, 32] the unloaded Q was extracted from the reflection data.

Figure 9 shows a plot of the unloaded Q values against temperature for the superconducting and an identical gold (Au) resonator at 10.4 and 20.2 GHz. The Q values of the Au resonator are relatively flat over this temperature range with the Q values at 20.2 GHz larger than those at 10.2 GHz, as expected for a conductor loss-limited transmission line resonator where $Q \propto f^{1/2}$, and f is the frequency. A measurable response for the HTS resonators began just below the $T_c(R = 0)$ value measured for the films. As seen in figure 9, the Q values increased with decreasing temperature and exceeded the Q values of the Au resonator around 60 to 65 K. However, the BSCCO unloaded Q values above $\sim$60 K

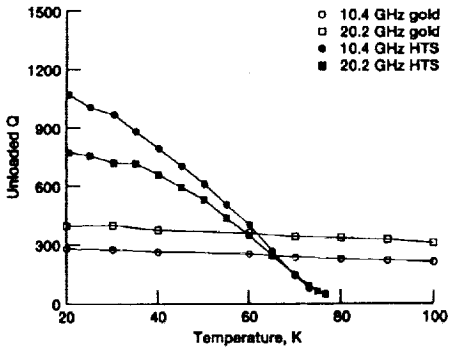

Figure 9. Linear resonator unloaded Q values for BSCCO HTS and gold strips.

are less than those for the Au resonator because the thinner BSCCO film (0.3 μm for BSCCO; 1.5 μm for Au) leads to overall higher conductor loss and lower Q. The Q values of the superconducting resonator kept increasing down to the lowest temperatures measured, reaching values of approximately four times that of the Au circuit Q at 10.4 GHz and 20 K, and approximately twice that of the Au circuit Q at 20.2 GHz and 20 K. It should be noted that for the superconducting resonator the 10.4 GHz resonance has a higher Q than the 20.2 GHz resonance, contrary to the observations for the Au resonator. This is due to the $R_s \propto f^2$ dependence for the superconducting film which leads to $Q \propto 1/f$ for a conductor loss-limited transmission line resonator.

The unloaded Q values of the resonator may be used to estimate the R_s of the BSCCO thin film [32]. The R_s values obtained at 10.4 and 20.2 GHz, and the R_s values corresponding to Au are plotted in figure 10. R_s values at 73 K of 13 and 22 mΩ were obtained for the BSCCO at 10.4 and 20.2 GHz respectively. At 20 K, R_s was $\sim$0.75 and 2.9 mΩ at 10.4 and 20.2 GHz respectively. These R_s values are less than those for the Au film at the same frequencies and temperatures, and are approximately eight times smaller than earlier values ($\sim$25 mΩ at 25 K) reported at 7 GHz [29]. Also plotted in figure 10 are the values of R_s for the BSCCO thin film at 20.2 GHz obtained assuming a $R_s \propto f^2$ dependence, where f is the frequency, and using the experimental values measured at 10.4 GHz. Note that although there is a noticeable discrepancy between the measured and calculated R_s values at 20.2 GHz at T near T_c, the agreement between the two sets of values improves at temperatures far below T_c.

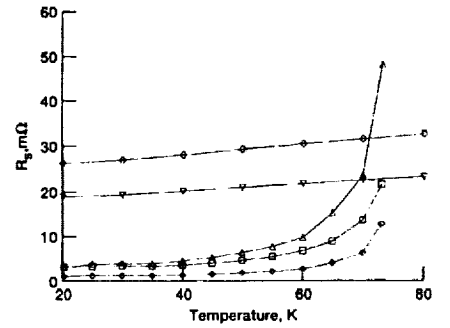

Figure 10. Surface resistance, R_s, for BSCCO HTS strip at 10.4 GHz (◇) and 20.2 GHz (□). The R_s of a gold strip at 10.4 (▽) and 20.2 (○) GHz are shown for comparison purposes. Also shown is the R_s for the BSCCO HTS strip at 20.2 GHz calculated from the measured R_s at 10.4 GHz assuming an $R_s \propto f^2$ dependence (△).

4. Discussion

We have characterized co-evaporated BSCCO thin films on $SrTiO_3$ and $LaAlO_3$ substrates. We have compared the films in terms of their T_c and J_c values, surface morphology and XRD patterns. It was observed that, although both films have similar DC T_c, the film on the $SrTiO_3$ substrate has a larger J_c from 4.2 to 40 K, a smoother surface morphology, and lower R_s than its counterpart on $LaAlO_3$. From the power transmission measurements we have shown that the conductivity in the superconducting state does not follow either the BCS or two-fluid model temperature dependence. However, the observed increase in σ_1 for $T < T_c$ is consistent with the observation of Ho *et al* [20] (for ion-beam-deposited BSCCO thin films on MgO at 60 GHz) who suggested that this trend below T_c is either an intrinsic temperature dependence of the homogeneous superconductor or the manifestation of the response of a composite consisting of superconducting regions growing in a normal conducting matrix. In the case of our films, although σ_1 increases very quickly upon cooling the sample below $\sim$88 K, we also observed that, contrary to the observations by Ho *et al* [20], it reaches a maximum at T not far below T_c^{mw} and then falls very quickly. This behaviour may be due to the better quality of the co-evaporated films under study as compared with those analysed by Ho *et al* [20], which have $T_c \sim 68$ K and $J_c \sim 5 \times 10^4$ A cm^{-2} at 10 K. Thus it may be reasonable to assume that as the quality of the material improves, i.e., as the normal conductor fraction in the material decreases, the behaviour below T_c could actually approach that expected from the two-fluid model. A more rigorous analysis should be performed along this line in the future.

From the R_s values obtained using the resonant cavity technique, one can see that the values at 77 K for the films on $SrTiO_3$ and $LaAlO_3$ are approximately 12 and 20 times, respectively, larger than those of pure Cu and Au at room temperature, and about 8 and 13 times, respectively, that of a Au-plated Cu sample. However, the R_s measured at 10.4 GHz using the linear resonator patterned on the film on $LaAlO_3$ ($\sim$13 mΩ) is similar to that of pure Cu and pure Au at the same frequency and temperature ($R_{s,Cu} \sim 10$ mΩ, $R_{s,Au} \sim 14.3$ mΩ), and lower than that of its Au counterpart ($\sim$23 mΩ). We

found that when the $R_s \propto f^2$ dependence was used to determine the R_s of the BSCCO film at 20.2 GHz using the resonator technique, the agreement between the calculated and measured values at this frequency improved for temperatures far from T_c. However, when the same approach was used to determine the R_s at 58.9 GHz ($R_s \sim 13$ mΩ at 10.4 GHz, and ~ 417 mΩ at 58.9 GHz) the resulting value was approximately one-third of that obtained by the cavity technique at temperatures near 77 K, the discrepancy becoming worse for lower temperatures. This deviation is not unexpected since we are dealing with an heterogeneous system in which the different components (superconducting, normal and possibly insulating) do not necessarily respond to frequency changes in the same way and therefore may alter the frequency dependence of the microwave losses that one expects for a homogeneous superconductor. In addition it will be interesting to see how the different measurement techniques contribute to the deviation especially when it has been suggested by others that calibration differences in different techniques to measure R_s can contribute to the lack of correlation between R_s values in HTS thin films [33].

We have also obtained λ for the BSCCO films under discussion. Low temperature values for $\lambda \sim 1.0$ μm were obtained. Although these values compare favourably with those obtained by others in BSCCO films, they are still approximately three times the values reported by others for BSCCO single crystals. This may be due to the inhomogeneity of the films under study as shown by the unknown peaks observed in the XRD pattern (figure 3). It has been shown by others that non-superconducting inclusions and weak link effects result in an increase of λ [34]. The fact that the low temperature λ is large compared with the values typically obtained at low temperatures for YBCO thin films ($\sim$0.14–0.3 μm) [5–7] may impose limitations in the use of this type of BSCCO thin film for microwave applications. In normal conductors, in order to have low conductor losses, the conductor thickness must be at least three times larger than the normal skin depth (δ). If, as in the YBCO films, the superconducting properties of the BSCCO films deteriorate as the film thickness goes beyond 0.5 μm, then it is clear that improvements in the BSCCO film growth are still necessary. Therefore careful study of the various microwave transmission lines, in terms of the contribution to total losses (i.e., conductor, substrate and radiation losses [35]) must be performed to determine, in view of the limitations described above, for which of these structures the BSCCO HTS film would be more suitable.

Nevertheless, since the values of T_c and J_c compared well with those of other BSCCO thin films deposited by other techniques, we believe that the microwave data presented here are representative of state-of-the-art BSCCO films. In view of this we can see that this type of film offers some possibilities for microwave applications at low frequencies (i.e., $\leqslant$20 GHz), but potential applications at frequencies around 60 GHz and above will require further improvements in the material.

5. Conclusions

We have characterized co-evaporated BSCCO thin films on $SrTiO_3$ and $LaAlO_3$. The J_c values measured for these films are better than or equal to those reported by others for state-of-the-art BSCCO films deposited by other techniques. From the microwave power transmission measurements we were able to determine σ^*; it was found that the temperature dependence of σ^* for $T < T_c$ deviates from both the BCS theory and the two-fluid model. The low temperature values of λ agreed with those reported by others for BSCCO films, but were approximately three times larger than those of BSCCO single crystals. R_s values for the BSCCO thin films were measured at 10.4, 20.2, and 58.9 GHz. From the R_s data it is evident that the low-T_c phase BSCCO thin films could offer possibilities for microwave applications at low frequencies ($\leqslant$20 GHz), but applications at frequencies around 60 GHz and above will require further improvements in the material. To our knowledge this is the first time a microwave characterization in terms of the transport parameters most relevant for transmission line applications has been performed on the same BSCCO film and in the frequency range from 10 to 60 GHz.

Acknowledgments

The authors would like to thank Ms Ruth Cipcic and Mr Ralph Garlick for the x-ray-diffraction measurements. The assistance of D Bohmann in obtaining the SEM micrographs of the films and measuring their thickness is deeply appreciated. We thank Ms C Cubbage for her assistance in measurements of the gold linear resonator. Finally we thank Dr V O Heinen for helpful discussions and suggestions.

References

[1] Klein N, Muller G, Piel H, Roas B, Schultz L, Klein U and Peiniger M 1989 *Appl. Phys. Lett.* **54** 757

[2] Drabeck L, Gruner G, Chang J J, Inam A, Wu X D, Nazar L, Venkatesan T and Scalapino D J 1989 *Phys. Rev. B* **40** 7350

[3] Harshman D R, Schneemeyer L F, Waszczak J V, Aeppli G, Cava R J, Batlogg B, Rupp L W, Ansaldo E J and Williams D L 1989 *Phys. Rev.* B **39** 851

[4] Qui X G, Cui C G, Zhang Y Z, Li S L, Zhao Y Y, Xu P and Li L 1990 *J. Appl. Phys.* **68** 884

[5] Anlage S M, Langley B W, Deutscher G, Halbritter J and Beasley M R 1991 *J. Phys. Rev.* B **44** 9764

[6] Kobrin P H, Ho W, Hall W F, Hood P J, Gergis I S and Harker A B 1990 *Phys. Rev.* B **42** 6259

[7] Miranda F A, Gordon W L, Bhasin K B, Heinen V O and Warner J D 1991 *J. Appl. Phys.* **70** 5450

[8] Maeda H, Tanaka Y, Fukutomi M and Asano T 1988 *Japan. J. Appl. Phys.* **27** L209
[9] Talvacchio J, Wagner G R and Talisa S H 1991 *Microwave J.* **34** 105
[10] Miranda F A, Bhasin K B, Heinen V O, Kwor R and Kalkur T S 1990 *Physica* C **168** 91
[11] Kalkur T S, Kwor R Y, Jernigan S and Smith R 1989 *Science and Technology of Thin Film Superconductors* ed R D McConnell and S A Wolf (New York: Plenum) p 487
[12] Narumi E, Lee J, Li C, Hosokawa S, Patel S and Shaw D T 1991 *Appl. Phys. Lett.* **59** 3180
[13] Xi X X *et al* 1991 *IEEE Trans. Magn.* **MAG-27** 982
[14] Yeh J J and Hong M 1989 *Appl. Phys. Lett.* **54** 769
[15] Bean C P 1962 *Phys. Rev. Lett.* **8** 250
[16] Gorshunov B P, Kozlov G V, Krasnosvobodtsev S I, Pechen E V, Prokhorov A M, Prokhorov A S, Syrotynsky O I and Volkov A A 1988 *Physica* C **153–154** 667
[17] Weaver H E 1959 *J. Phys. Chem. Solids* **11** 274
[18] Miranda F A, Gordon W L, Bhasin K B, Ebihara B T, Heinen V O and Chorey C M 1990 *Microwave Opt. Tech. Lett.* **3** 11
[19] Simon R W, Platt C E, Lee A E, Lee G S, Daly K P, Wire M S, Luine J A and Urbanik M 1988 *Appl. Phys. Lett.* **53** 2677
[20] Ho W, Hood P J, Hall W F, Kobrin P, Harker A B and DeWames R E 1988 *Phys. Rev.* B **38** 7029
[21] Kobrin P H, Ho W, Hall W F, Hood P J, Gergis I S and Harker A B 1990 *Phys. Rev.* B **42** 6259
[22] Hinken J H 1989 *Superconductor Electronics: Fundamentals and Microwave Applications* (Berlin: Springer)
[23] Tinkham M 1980 *Introduction to Superconductivity* (New York: McGraw-Hill)
[24] Byrne D P, Kwor R Y and Kalkur T S 1991 *J. Appl. Phys.* **69** 6693
[25] Mitra S, Cho J H, Lee W C, Johnston D C and Kogan V G 1989 *Phys. Rev.* B **40** 2674
[26] Gygax S, Xing W, Rajora O and Curzon A 1989 *Physica* C **162–164** 1551
[27] Ansaldo E J, Batlogg B, Cava R J, Harshman D R, Rupp L W, Riseman T M and Williams D 1989 *Physica* C **162–164** 259
[28] Miranda F A, Gordon W L, Bhasin K B and Warner J D 1990 *Appl. Phys. Lett.* **57** 1058
[29] Lichtenberg C L, Wosik J, Davis M and Wolfe J C 1989 *NASA TM-102159*
[30] Andreone A, Attanasio C, Dichiara A, Maritato L, Nigro A, Peluso G and Vaglio R 1991 *Physica* C **180** 272
[31] Ginzton E L 1957 *Microwave Measurements* (New York: McGraw-Hill)
[32] Chorey C M, Kong K S, Bhasin K B, Warner J D and Itoh T 1991 *IEEE Trans. Microwave Theory Tech.* **39** 1480
[33] Talvacchio J and Wagner G R 1990 *SPIE Proc.* **1292** 2
[34] Hylton T L, Kapitulnik A, Beasly M R, Carini J P, Drabeck L and Gruner G 1988 *Appl. Phys. Lett.* **53** 1343
[35] Kong K S, Bhasin K B and Itoh T 1991 *SPIE Proc.* **1477** 57

PROCESSING, ELECTRICAL AND MICROWAVE PROPERTIES OF SPUTTERED Tl-Ca-Ba-Cu-O SUPERCONDUCTING THIN FILMS

G. Subramanyam and V. J. Kapoor
Department of Electrical & Computer Engineering
University of Cincinnati
Cincinnati, OH 45221-0030

C. M. Chorey
Sverdrup Technology Inc. (NASA Lewis Group)
Cleveland, OH 44135

K. B. Bhasin
NASA Lewis Research Center
Cleveland, OH 44135

Abstract--A reproducible fabrication process has been established for TlCaBaCuO thin films on $LaAlO_3$ substrates by rf magnetron sputtering and post-deposition processing methods. Electrical transport properties of the thin films were measured on patterned four-probe test devices. Microwave properties of the films were obtained from unloaded Q measurements of all-superconducting ring resonators. This paper describes the processing, electrical and microwave properties of $Tl_2Ca_1Ba_2Cu_2O_x$ (2122) phase thin films.

I.INTRODUCTION

The high temperature superconducting thin films show great promise for electronic applications at 77 °K. Since the discovery of high T_c materials, there has been a substantial progress in the applications such as SQUIDs, passive microwave devices, IR detectors and interconnections in microelectronics. Among the high T_c materials, the TlCaBaCuO compound has proven to possess the highest T_c of 125 °K[1], and hence offers a wide margin of temperature range for applications at 77 °K. Thin films of TlCaBaCuO compound have shown T_c as high as 120 °K, and critical current density (J_c) greater than 10^6 A/cm^2 at 77 K[2]. Also, TlCaBaCuO thin films, primarily of 2122 phase have shown surface resistance (R_s) about 80 times lower than Cu at 10 GHz and 77 °K[3]. This research work primarily addresses a reproducible processing method for TlCaBaCuO thin films of 2122 phase, electrical transport measurements and also microwave ring resonator measurements.

This research was supported by NASA Lewis Research Center.
Manuscript received August 24, 1992.

II.PROCESSING OF TlCaBaCuO THIN FILMS

The TlCaBaCuO thin films were sputter deposited on (100) $LaAlO_3$ substrates from a single composite powder target in a CVC model 601 rf magnetron sputtering system. The target was a Tl enriched $Tl_2Ca_2Ba_2Cu_3O_x$ (2223) powder target, with 20% excess Tl_2O_3 to compensate for the loss of Tl during post-processing steps and to maintain sufficient composition for several deposition runs. The sputter depositions were performed at an rf power density of 0.7 W/cm^2, and the chamber pressure at 5 mTorr, in a pure argon atmosphere. The thin films were deposited at a deposition rate of approximately 30 Å/min. The sputter deposited thin films of 0.3-0.5 μm thickness were post-processed in two steps: first, sintering in air at 850 °C for 12-15 minutes in an optimum Tl_2O partial pressure, and the second, annealing in oxygen flow at 750 °C. These steps were performed in a box furnace with samples placed in an enclosed platinum crucible. The Tl_2O partial pressure was provided by placing 2223 pellets inside the crucible. Both the steps were performed with the same number of pellets placed inside the crucible. The Tl_2O partial pressure provided during the sintering process establishes the phase in the thin films. The details of the post-processing steps have been reported earlier[4-5].

To provide the optimum Tl_2O partial pressure during the post-processing steps, a simple technique was used to monitor the reduction in Tl content in the as-deposited thin films, after each sputtering run. Percentage reduction in Tl content from run to run was obtained by Auger Electron Spectroscopy(AES) surface analysis on the as-deposited samples. This percentage reduction in Tl gives an approximate estimate of additional Tl_2O partial pressure needed for the post-deposition processes. The estimated additional Tl_2O partial pressure was provided

by adding additional 2223 pellets in the crucible. This technique has yielded reproducible high T_c and high J_c thin films. The annealed thin films were essentially smooth in morphology. The superconducting thin films were characterized by X-ray diffraction(XRD) analysis to determine the phase purity. XRD spectra obtained on a TlCaBaCuO thin film is shown in figure 1. The characteristic peaks of 2122 and 2223 phases were present. The 2122 phase with c-axis oriented growth was the dominant phase in the thin films, as determined from the XRD data.

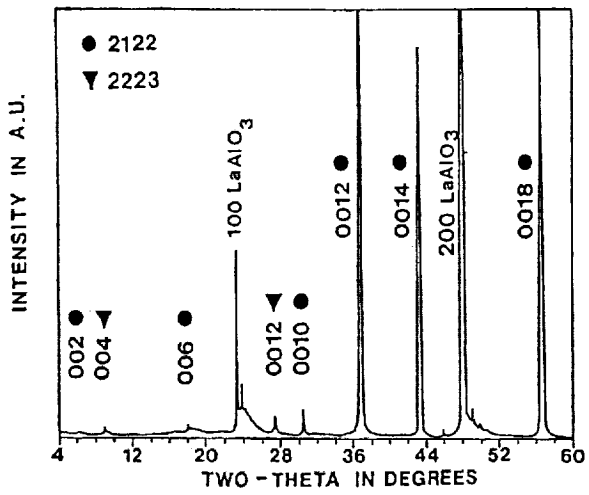

Fig.1 XRD spectra obtained on an annealed TlCaBaCuO thin film showing c-axis oriented 2122 and 2223 peaks.

III.ELECTRICAL TRANSPORT PROPERTIES

Electrical transport measurements were performed on patterned four-probe test devices 10, 25 and 50 μm wide, and 1 mm long. The test devices were patterned on as-deposited TlCaBaCuO thin films using standard positive photoresist photo-lithography, and wet chemical etching in a weak phosphoric acid. Positive photoresist AZ 1421 was used for the photo-lithography. The etching solution was a 1:100 phosphoric acid:DI H_2O heated to about 75 °C. The etch rate was approximately 30 Å/min. The patterned samples were post-processed using our standard procedures described above.

For reliable electrical measurements, a process for making low resistance gold contacts on TlCaBaCuO thin films was established. First, metal bonding pads were formed by thermally evaporating 6000 Å thick gold film on the superconducting pads of the four-probe device. The samples were annealed at 600 °C for 15 minutes in an oxygen flow of 1 liter/min, followed by a slow furnace cooling for 30 minutes after the furnace was switched off. Gold wires were bonded to the pads using an ultrasonic wedge bonder. Typically, the four-probe test devices showed zero resistance T_c between 97 and 100 °K. The measurements were performed at a constant applied current of 10 μA. The contact resistance obtained from the I-V measurements of the four-probe devices is typically a few mΩ at temperatures below Tc. The specific contact resistivity was approximately 3.65×10^{-5} Ω-cm^2 at 90 °K, and below 10^{-8} Ωcm^2 at 77 °K.

The zero-field transport current density (J_c) measurements were performed using dc and pulsed current techniques, using a 1 μV/mm electric field criterion. Figure 2 shows the J_c vs temperature measurements obtained on two four probe test devices. Zero-field J_c greater than 10^5 A/cm^2 at 77 °K was obtained in the four-probe devices tested.

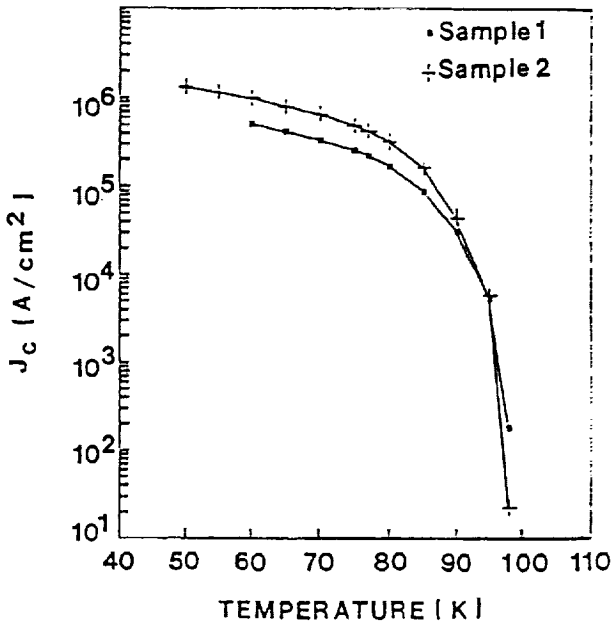

Fig.2 Zero-field J_c vs Temperature for two different TlCaBaCuO thin films measured using 1 μV/mm criterion.

III.MICROWAVE PROPERTIES

The microwave properties of the TlCaBaCuO thin films were obtained indirectly by measuring the unloaded Q of all-superconducting ring resonators. A ring resonator was designed for a fundamental resonance at 12 GHz. The device consisted of a ring structure separated from the feed line by a small coupling gap. The figure 3 shows a ring resonator designed for fundamental resonance at 12 GHz, for 10 mil

thick $LaAlO_3$ substrates(ϵ_r=24.5). In the figure, the linewidth of the ring and the microstrip feed line is W=5.6 mils, the coupling gap G=1.75 mils, and the mean radius of the ring R=77 mils.

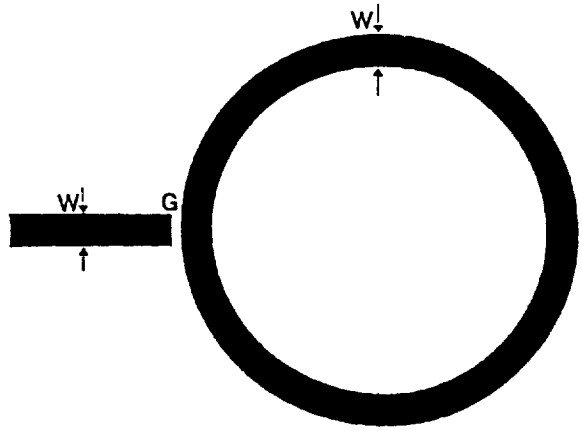

Fig.3 Microstrip ring resonator designed for 12 GHz

The TlCaBaCuO ring resonators were fabricated by patterning 0.3 μm thin films using AZ 1421 photolithography, and wet chemical etching techniques described before. After processing the top conductor side, the ground plane TlCaBaCuO thin film was deposited to a thickness of 0.3 μm, and post-processed using the same steps described in section II. The unloaded Q of the resonators were obtained by swept frequency reflection measurements[6] using a HP8720B network analyser. The unloaded Q versus temperature characteristics for an all-superconducting TlCaBaCuO ring resonator is shown in curve A of figure 4. For comparison, data for a gold resonator with gold ground plane is shown in curve B.

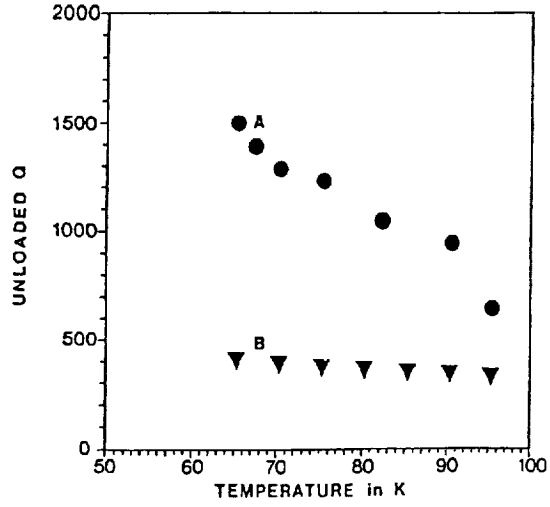

Fig.4 The unloaded Q vs temperature characteristics of an all-superconducting TlCaBaCuO ring resonator

The unloaded Q of the superconducting ring resonator is approximately four times higher than the gold resonator at 65 °K. The ring resonators offer an indirect method for measuring the surface resistance (R_s) of superconducting thin films. By separating the conductor and dielectric losses, the R_s of the TlCaBaCuO thin films were calculated using the standard microstrip loss equations described by Pucel et al[7]. The effective R_s at 12 GHz and 77 °K was determined to be typically between 1.5 and 2.75 mΩ, almost an order of magnitude lower than the R_s of Cu at the same frequency and temperature. The lowest surface resistance reported in $Tl_2Ca_1Ba_2Cu_2O_x$ thin films to date is 0.130 mΩ at 77 K and 10 GHz[3].

The swept frequency reflection measurements performed at several temperatures, were also used in determining the effective penetration depth in the TlCaBaCuO thin films. The shift in resonance frequency with temperature is mainly due to the temperature dependence of the penetration depth in the superconducting thin film. The phase velocity of a superconducting microstrip line with a superconducting ground plane is given by[8],

$$v_{ph} = c/\sqrt{\epsilon_{eff}}\{1+2(\lambda/h)\coth(t/\lambda)\}^{-0.5} \quad --(1)$$

where c is the velocity of light, ϵ_{eff} is the effective dielectric constant, h is the substrate thickness, t is the thickness of the microstrip, λ the penetration depth of the superconducting microstrip. The penetration depth is temperature dependent based on the Gorter-Casimir relationship, ie.,

$$\lambda(T) = \lambda(0)[1-(T/Tc)^4]^{-0.5} \quad --(2)$$

for temperature T less than Tc. $\lambda(0)$ is the penetration depth at T=0 °K. The resonance frequency of the ring resonator is given by the equation

$$f = nv_{ph}/(2L) \quad --(3)$$

where f is in GHz, L is the mean circumference of the ring in mm, and n is the integer order of resonance. From the above equations, the lowest value of the effective $\lambda(0)$ was determined to be 6890 Å. The typical value ranges between 7000 Å and 8000 Å. Since the thin films were only 0.3-0.4 μm thick, the penetration depth depends upon the properties of the superconductor through the entire film. This may be a reason for the higher penetration depth. The typical values of penetration depth reported in literature is between 4000 and 8000 Å in Tl 2122 phase thin films[9-10]. The higher value of penetration depth is also an indication of the film quality. Improvements in film quality should yield lower effective

penetration depth and lower R_s values.

IV.SUMMARY

A reproducible fabrication process has been established for TlCaBaCuO thin films of 2122 phase on $LaAlO_3$ substrates. Zero resistance T_c as high as 100 °K, and the zero-field J_c as high as $5x10^5$ A/cm^2 were obtained in four-probe test devices. The surface resistance of the TlCaBaCuO thin films obtained by separating the conductor losses from Q measurements in ring resonators is typically between 1.5 and 2.75 mΩ at 12 GHz and 77 °K. The effective penetration depth at 0 °K, calculated from the resonance frequency shift with temperature measurements was typically between 7000 and 8000 Å.

REFERENCES

[1] S. S. P. Parkin, V. Y. Lee, E. M. Engler, A. I. Nazzal, T. C. Huang, G. Gorman, R. Savoy and R. Beyers,"Bulk superconductivity at 125 °K in $Tl_2Ca_2Ba_2Cu_3O_x$", Phys. Rev. Lett., vol.60, pp 2539-42, 1988.

[2] W. Y. Lee, S. M. Garrison, M. Kawasaki, E. L. Venturini, B. T. Ahn, R. Boyers, J. Salem, R. Savoy, and J. Vasquez, "Low temperature formation of epitaxial $Tl_2Ca_2Ba_2Cu_3O_{10}$ thin films in reduced O_2 pressure", Appl. Phys. Lett., vol.60, pp 772-774, 1992.

[3] W. L. Holstein, L. A. Parisi, C. Wilker, and R. B. Flippen, "$Tl_2Ba_2Ca_1Cu_2O_8$ films with very low microwave surface resistance up to 95 K", Appl. Phys. Lett., vol.60, pp 2014-2016, 1992.

[4] D. S. Ginley, J. F. Kwak, E. L. Venturini, B. Morosin, and R. J. Baughman, "Morphology control and high critical currents in superconducting thin films in the TlCaBaCuO system", Physica C, vol.160, pp 42-48, 1989.

[5] G. Subramanyam, F. Radpour, V. J. Kapoor, and G. H. Lemon, "Fabrication and chemical composition of rf magnetron sputtered TlCaBaCuO high Tc thin films", J. Appl. Phys. vol.68, pp 1157-63, 1990.

[6] J. Aitken, "Swept frequency microwave Q factor measurements", Proc. of Inst. Elec. Eng. vol.123, pp 855-862, 1976.

[7] R. A. Pucel, D. J. Masse, and C. P. Hartwig, "Losses in microstrip", IEEE Trans. Microwave Theory Tech., vol.16, pp 342-350, 1968. Also "Correction to losses in microstrip", IEEE Microwave Theory Tech., vol.16, pp 1064, 1968.

[8] R. L. Kautz, "Picosecond pulses on superconducting strips", J. Appl. Phys. vol.49, pp 308-314, 1978.

[9] V. M. Hietala, J. S. Martens, D. S. Ginley, T. E. Zipperian, C. P. Tigges, M. S. Housel, and T. A. Plut, "Evaluation of superconducting Tl-Ca-Ba-Cu-O thin film surface resistance using a microstrip ring resonator", IEEE Microwave and Guided Wave Lett., vol.1, pp 84-86, 1991.

[10] Private Communications with Dr. Felix A. Miranda of NASA Lewis Research Center.

Electrical-transport properties and microwave device performance of sputtered TlCaBaCuO superconducting thin films

G. Subramanyam and V. J. Kapoor
Microwave Electronics Laboratory, Department of Electrical and Computer Engineering, University of Cincinnati, Cincinnati, Ohio 45221-0030

C. M. Chorey
Sverdrup Technology Inc., NASA Lewis Group, Cleveland, Ohio 44135

K. B. Bhasin
NASA Lewis Research Center, Cleveland, Ohio 44135

(Received 21 February 1991; accepted for publication 1 June 1992)

Tl-Ca-Ba-Cu-O high-temperature superconducting thin films were deposited on lanthanum aluminate substrates, by rf magnetron sputtering and postannealing methods. A reproducible fabrication process with low-resistance metal contacts has been established for high-T_c and high-J_c TlCaBaCuO thin films after patterning using standard microelectronic photolithography and wet chemical etching techniques. Low-resistance gold contacts on TlCaBaCuO thin films were obtained by annealing in an oxygen flow of 1 l/min followed by a slow furnace cooling. Specific contact resistivity was approximately 10^{-10} $\Omega\,cm^2$ below 77 K. High transition temperatures as high as 100 K, and current density at zero magnetic field greater than 10^5 A/cm^2 are routinely obtained in 0.3–0.5 μm TlCaBaCuO thin films. The morphology studies of the films using scanning electron microscopy show the correlation between J_c and the microstructure of the films. Films with featureless morphology have larger zero-field transport currents. The microwave properties of TlCaBaCuO thin films were investigated by designing, fabricating, and characterizing microstrip ring resonators with a fundamental resonance frequency of 12 GHz on 10-mil-thick lanthanum aluminate ($LaAlO_3$) substrates. Ring resonators with a superconducting ground plane of 0.3 μm thickness and a gold ground plane of 1 μm thickness were fabricated and characterized in the temperature range of 60–95 K. Typical unloaded quality factors Q for the ring resonators at 12 GHz were above 1500 at 65 K, compared to an unloaded Q of 370 for a gold ring resonator. A surface resistance as low as 1.5 mΩ at 12 GHz and 77 K was obtained in 0.3 μm TlCaBaCuO thin films using the ring resonator Q measurements. Typical values of penetration depth at 0 K in the TlCaBaCuO thin films were determined to be between 7000 and 8000 Å using the temperature variation of resonance frequency measurements.

I. INTRODUCTION

Since the discovery of a copper-oxide high transition temperature (T_c) superconductor by Bednorz and Muller in January 1986,[1] there has been substantial progress in superconducting electronics. Several new compounds such as YBaCuO,[2] BiSrCaCuO,[3] and TlCaBaCuO (Ref. 4) have been found to be superconducting above 90 K, thus making it feasible for electronic applications at liquid-nitrogen temperature (77 K). Currently, worldwide research is underway for developing high-T_c superconducting electronics. Already rapid progress has been made for applications of high-T_c materials in areas such as superconducting quantum interference devices (SQUIDs), passive microwave devices, IR detectors, and interconnections in microelectronics.[5–8]

Among the high-T_c materials, the TlCaBaCuO compound has proven to possess the highest T_c[9] which means a wide margin of operational range is available for electronic applications at 77 K. The TlCaBaCuO thin films are very attractive for electronic applications, as they have shown high T_c and high critical current density J_c.[10,11] Fabrication of TlCaBaCuO thin films on lanthanum aluminate ($LaAlO_3$) substrates has been reported by the authors.[12–14] $LaAlO_3$ substrates have a good a-axis lattice match with TlCaBaCuO thin films to permit highly c-axis-oriented growth of TlCaBaCuO superconducting thin films. The dielectric constant of $LaAlO_3$ is 24.5 (Ref. 15) and the loss tangent is approximately 8.3×10^{-5} at 77 K.[15] The growth of TlCaBaCuO thin films on $LaAlO_3$ substrates offers promising applications in the area of microwave electronics. The only disadvantage of TlCaBaCuO compound is the toxicity of thallium (Tl) which needs very careful processing and handling procedures. For microelectronic and microwave applications of TlCaBaCuO thin films, it is very important to establish a reproducible fabrication process for superior electrical and microwave properties.

The foremost applications of high-T_c thin films is expected to be in the area of "passive microwave devices" such as resonators and filters. High-T_c superconducting thin films have lower surface resistance R_s compared to Cu and Au, corresponding to higher Q and improved performance in passive microwave devices. TlCaBaCuO thin-film-based passive microwave devices have shown superior

performances. Chang *et al.*[5] have reported a surface resistance at least an order smaller than Cu at 77 K and 9.5 GHz. Bourne *et al.*[6] reported a 1 ns microstrip delay line using thin films of TlCaBaCuO, again a factor of 10 improvement in loss was observed at 3.29 GHz and 77 K. Hammond *et al.*[7] reported a TlCaBaCuO microstrip resonator and its power handling performance at 77 K. At effective power levels in the resonator up to 100 W, the Q was still three times higher than a silver resonator at 2.6, 5.2, and 7.3 GHz. Linear resonators with loaded Q as high as 15 000 at 5 GHz have been demonstrated.[8]

This paper describes the processing and electrical transport measurements for achieving reproducible high-T_c, high current density J_c, low microwave surface resistance R_s TlCaBaCuO thin films on $LaAlO_3$ substrates, for microelectronic applications. A method for fabricating low-resistance contacts on TlCaBaCuO thin films for reliable electrical transport measurements is also addressed. The microwave properties of TlCaBaCuO thin films were investigated by designing, fabricating, and characterizing microstrip ring resonators for 12 GHz fundamental resonance frequency. This paper describes the results of these investigations.

II. EXPERIMENTAL

TlCaBaCuO thin films were sputter deposited from a single composite powder target in a CVC model 601 rf sputtering system operating at 13.56 MHz. The system was operated in the rf magnetron mode to improve the sputtering yields at low working pressures. The depositions were performed in a "sputter up" configuration on substrates placed face down. The $Tl_2Ca_2Ba_2Cu_3O_x$ powder target was prepared by the solid-state reaction of stoichiometric amounts of high-purity BaO, CaO, CuO, and Tl_2O_3 (in the ratio 2:2:2:3) powders. The target was enriched with 20% excess Tl_2O_3 to compensate for the loss of Tl during the postprocessing of the thin films, and to maintain sufficient composition for several deposition runs. The powder target was spread over an 8-in.-diam copper plate which was part of the cathode assembly, and pressed to obtain a uniform surface. The (100) $LaAlO_3$ substrates were degreased in acetone, methanol, rinsed in de-ionized (DI) water, and blown dry using nitrogen before loading into the vacuum chamber. Depositions were performed at a rf power density of 0.7 W/cm^2, and a chamber pressure at 5 mTorr, in a pure argon atmosphere. The thin films were deposited to a thickness of about 3000–5000 Å, at a deposition rate of approximately 30 Å/min, as determined by Dektak profilometer thickness measurements. The detailed fabrication process has been described earlier by the authors.[12]

The sputter-deposited thin films of 0.3–0.5 μm thickness were postprocessed in two steps: first, sintering in air at 850 °C (to create the Tl_2O liquid phase), in an excess Tl partial pressure; and second, annealing in flowing oxygen at about 750 °C in an excess Tl partial pressure. These processes were performed in a small box furnace with the samples placed in an enclosed platinum crucible in the free-surface configuration described by Ginley *et al.*[11]

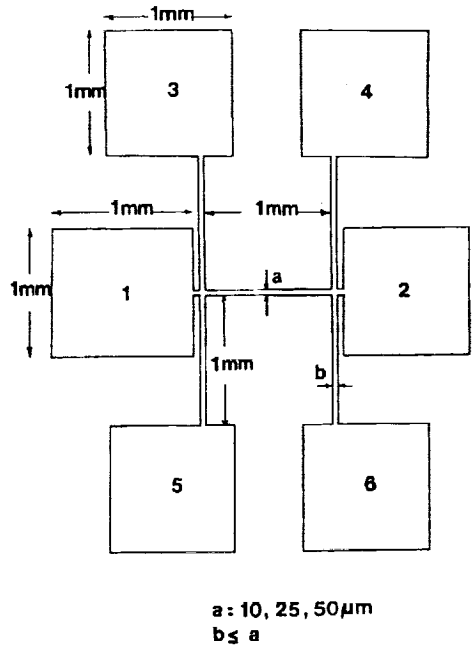

FIG. 1. The geometry of four-probe test devices with linewidths of 10, 25, and 50 μm for electrical-transport measurements. The voltage sense lines are 1 mm apart.

The thin films were placed on a $Tl_2Ca_2Ba_2Cu_3O_X$ pellet, with the film side facing the free surface in an enclosed platinum crucible. A second pellet was placed on a platinum wire mesh, approximately half an inch above the thin-film surface. The pellets provided the excess Tl partial pressure inside the crucible, mainly to minimize the loss of Tl from the thin films. The details of the post-processing heat treatments has been reported earlier.[11,12] For reproducible processing of TlCaBaCuO thin films, it was necessary to provide the optimum Tl partial pressure during postdeposition processes. A simple technique was used to monitor the reduction in Tl content in the as-deposited thin films, after each sputtering run. The percentage reduction in Tl content from run to run was obtained through Auger electron spectroscopy (AES) surface analysis on the as-deposited samples. The percentage reduction in Tl content compared to a standard reference 2223 pellet gives an approximate estimate of additional Tl partial pressure needed during the postdeposition processes. The estimated additional Tl partial pressure was provided for the postdeposition processes by adding additional 2223 pellets in the crucible. This technique has yielded reproducible high-T_c and high-J_c films.[14]

For the electrical-transport measurements, four-probe test devices were designed with linewidths of 10, 25, and 50 μm. The geometry of the test devices is shown in Fig. 1. The voltage sense lines were 1 mm apart, and the width of the sense lines was less than the linewidths in order to approximate a point contact as closely as possible. The test devices were patterned on as-deposited TlCaBaCuO thin films using standard photolithography and wet chemical

etching techniques. Positive photoresist AZ 1421 was used for the lithography. The as-deposited TlCaBaCuO thin films on $LaAlO_3$ substrates were prebaked at 180 °C for 20 min before the photoresist was spun. The photoresist AZ 1421 was spun on to a thickness of about 1 μm. The samples were soft baked at 90 °C for 20 min, followed by exposure to UV light in a mask aligner. The photoresist was developed in a 1:5 developer:DI H_2O solution for 45 sec. The samples were postbaked at 85 °C for 15 min to complete the photolithography process. A 1:90 phosphoric acid:DI H_2O solution was used for chemically etching the films. The solution was kept at a constant temperature of 75 °C. The etch rate was approximately 40 Å/min. After the etching process was completed, the photoresist was removed by immersing the samples in acetone for 25 s, followed by a 30 s rinse in DI H_2O. The patterned samples were postprocessed using our standard methods described above.

For electrical measurements on the test devices, metal bonding pads were formed by thermally evaporating 6000-Å-thick gold film on the superconducting pads, through a shadow mask. In order to obtain low-resistance contacts, the samples were annealed in an oxygen flow of 1 l/min, for about 15 min at 600 °C, followed by slow furnace cooling for 30 min after the furnace was switched off. The samples were removed when the furnace temperature was approximately 300 °C. Gold wires of 1 mil diameter were bonded to the gold pads using a Kulicke and Soffa Model 4123 ultrasonic wedge bonder. The bonding process did not require sample heating. For redundancy, multiple bonds were attached on the contact pads.

The zero-resistance T_c of the test devices was determined by measuring the resistivity versus temperature characteristics. The critical transport J_c was measured using dc and pulsed-current techniques, using a 1 μV/mm electric-field criterion. A Keithley model 181 nanovoltmeter and a Keithley model 224 current source were used for the dc transport measurements. The specimen temperature was controlled using a Lakeshore model 805 temperature controller, connected to a closed-cycle helium gas refrigeration system. The error in temperature measurement was less than 0.25 K. Thermal equilibrium was established before measurements at each temperature below T_c. The dc current method was not used above a current density of 10^4 A/cm^2, since sample heating at higher currents could cause the films to crack before measurements could be completed.

The pulsed current measurements were performed using two EG&G PARC 5210 lock-in amplifiers, a HP 214B pulse generator, and an adjustable current source capable of supplying 1 A. The pulse generator supplies a 10 V, 1 KHz pulse train with a 10% duty cycle. The pulsed current is applied to the test device, and the corresponding voltage pulse is measured across the sample using the lock-in amplifiers. The amplitude of the current pulse at which the voltage across the sample exceeds 1 μV yields the critical current at a particular temperature. The pulsed current measurements were compared to the dc values at as many temperatures as possible to insure the accuracy and compatibility of the two methods. The morphology of the finished TlCaBaCuO devices was examined in an ISI SX-30 scanning electron microscope (SEM). The morphology was evaluated in order to study the correlation between J_c and the microstructure of the films.

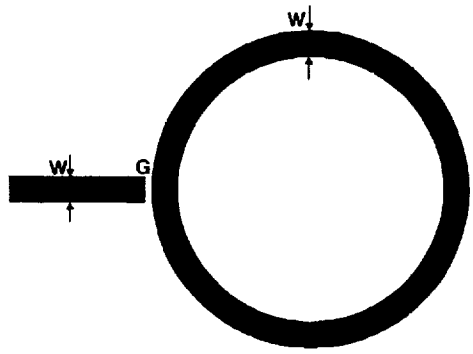

FIG. 2. Microstrip ring resonator designed for the fundamental resonance at 12 GHz. The coupling gap G and width W were chosen at 1.75 and 5.6 mils, respectively.

A microstrip resonator is a useful device for measurement of dispersion, phase velocity, and effective dielectric constants of dielectric substrates. Ring resonators are being widely used for realizing filters, and stabilization of oscillators. A microstrip ring structure resonates if its electrical length is an integral multiple of the guide wavelength. A simple ring resonator device was designed that consisted of a ring structure separated from the feed line by a small coupling gap. The size of the coupling gap determines the coupling between the feed line and the ring resonator. Loose coupling is desired to minimize excessive loading effects.[15] A ring resonator designed for 10-mil-thick $LaAlO_3$ substrates ($\epsilon r = 24.5$), for a fundamental resonance at 12 GHz is shown in Fig. 2. In the figure, the linewidth of the ring and the microstrip feed line is $W = 5.6$ mils, the coupling gap $G = 1.75$ mils, and the mean radius of the ring $R = (R1 + R2)/2 = 77$ mils. The characteristics impedance of the microstrip is 41 Ω at 12 GHz. The details of the design of the ring resonator have been described by Chorey *et al.*[15]

TlCaBaCuO ring resonators were fabricated by patterning 0.3 μm thin films using AZ 1421 positive photoresist photolithography and wet chemical etching techniques similar to the process used for fabricating the four-probe test devices described above. The ring resonators were annealed using the same annealing procedure described above. The samples were divided into two groups: one set of samples with 1 μm gold film on the bottom side of the $LaAlO_3$ substrate for the ground plane formation and a second set with a 0.3 μm TlCaBaCuO superconducting thin-film ground plane. The ground plane side superconductor was deposited and postprocessed using our routine postdeposition methods described above, after the microstrip ring resonator was fabricated on the top side.

A ring resonator was mounted in a gold-plated copper test fixture of 1 in. wide, 2 in. long, and 1 in. thick. The test

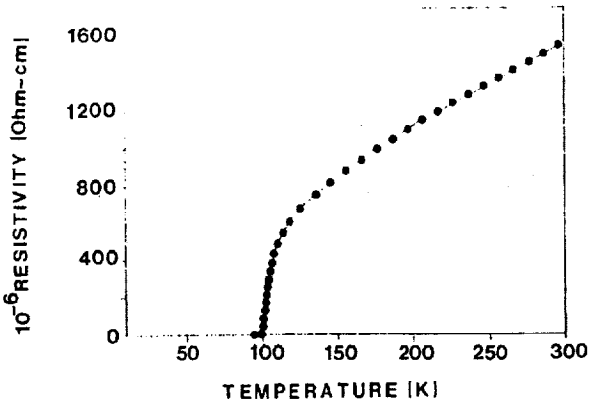

FIG. 3. The resistivity vs temperature characteristics of a patterned TlCaBaCuO thin-film test device, after lithography, chemical etching, and annealing, showing the onset of T_c at 106 K and zero resistivity at 98.5 K.

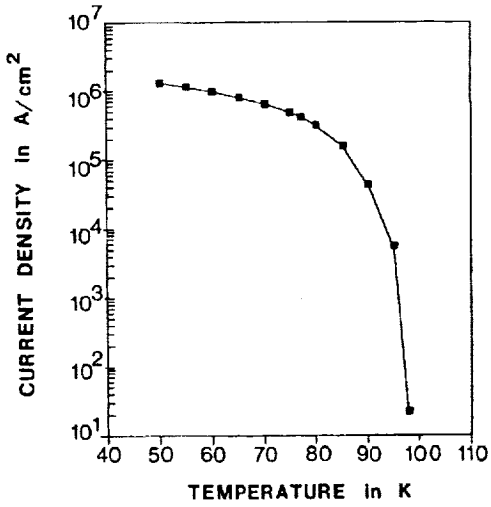

FIG. 4. Typical zero-field current density J_c vs temperature characteristics of a TlCaBaCuO four-probe test device obtained using the 1 μV/mm electric-field criterion.

fixture was placed on the cold head of the helium gas closed-cycle cryogenic system.[12] Electrical connection to the feed line was obtained by mechanical contact of a launcher at the input side of the test fixture. Connections to the HP 8720 network analyzer were made using a 0.141 in. semirigid coaxial cable of 50 Ω characteristic impedance. Before measurements were performed on ring resonators, standard one-port calibration was performed at room temperature. The calibration was performed using an open, a short, and a broadband load to effectively remove the test system imperfections introduced by the interconnecting cables, adapters, etc. The calibration was also valid at lower temperatures.

III. RESULTS

The resistivity versus temperature characteristics of a 50-μm-wide four-probe test device is shown in Fig. 3. The measurements were taken at a constant applied current of 10 μA. The onset of superconductivity occurred at 106 K, and the device showed zero resistance at 98.5 K. The room-temperature resistivity was 1.5×10^{-3} Ω cm. Zero resistance T_c between 97 and 100 K is routinely obtained. The T_c is low because of the $Tl_2Ca_1Ba_2Cu_2O_x$ (2122) phase, which is the dominant phase in these films. The thin films were also characterized by x-ray-diffraction analysis (XRD), and the results showed the characteristic peaks of 2122 and 2223 phases. The 2122 phase with c-axis-oriented growth was the dominant phase in the TlCaBaCuO thin films, as determined from the XRD data. The details of the XRD analysis are reported by the authors elsewhere.[13]

The contact resistance obtained from four-probe resistance measurements is typically a few mΩ, at temperatures below the T_c. The specific contact resistivity calculated from the four-probe resistance measurements range from 3.65×10^{-5} Ω cm^2 at 90 K, to 10^{-10} Ω cm^2 below 77 K. These results were reproducible from sample to sample and are comparable with the results for Au contacts on YBaCuO high-temperature superconducting thin films.

Figure 4 shows the typical zero-field current density J_c versus temperature measurements obtained on the four-probe test devices. Current densities at zero magnetic field as high as 5×10^5 A/cm^2 at 77 K an approximately 1×10^6 A/cm^2 at 60 K were obtained. The resistivity of the sample calculated from the I-V measurements is approximately 2.38×10^{-11} Ω cm at 77 K, much lower than any normal conductors at this temperature. The surface morphology of one of the test devices is shown in Fig. 5. The surface was essentially featureless and very smooth, typical of high-quality films. The current density of such films exceeded 10^5 A/cm^2 at 77 K. Films with numerous intergrain boundaries showed lower current densities below 10^4 A/cm^2 at 77 K.

The resonator quality factor Q, the ratio of the energy stored in the resonator to the energy dissipated in the resonator, was obtained from swept frequency reflection mea-

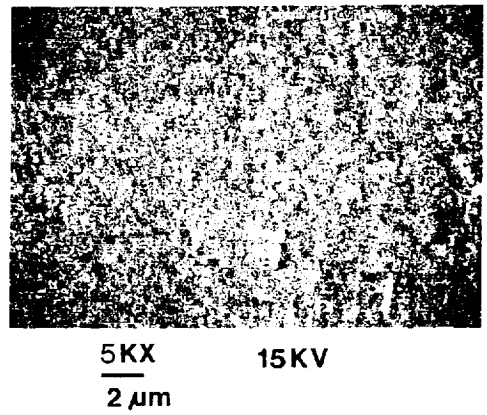

FIG. 5. Scanning electron micrograph of a TlCaBaCuO thin-film surface showing a smooth featureless morphology. The marker is 2 μm long.

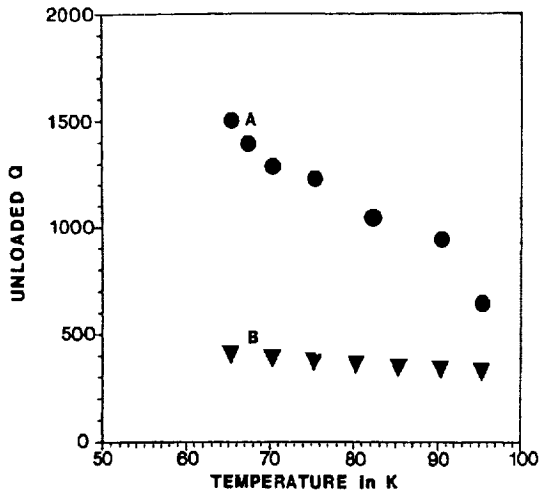

FIG. 6. The unloaded Q vs temperature characteristics of a TlCaBaCuO microstrip ring resonator. Curve A is for a superconducting ring resonator with a 0.3 μm TlCaBaCuO ground plane, and curve B is for a gold ring resonator.

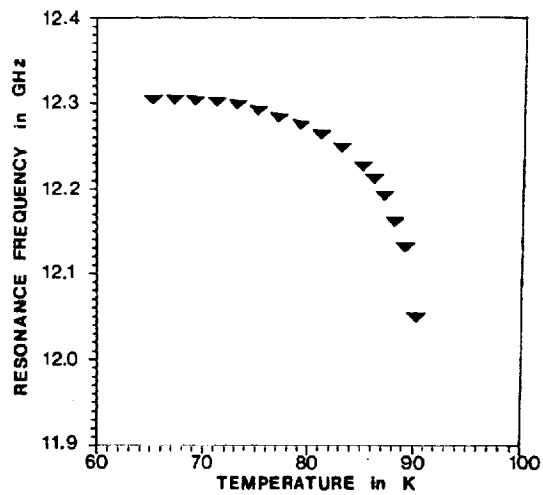

FIG. 7. The resonance frequency shift vs temperature characteristics of a TlCaBaCuO ring resonator.

surements.[15,16] The Q value is a figure of merit for a resonator, and is inversely proportional to the total losses in the circuit. The measured Q (called the loaded Q) is a measure of the circuit losses including the coupling loss and the loss through the feed line. The actual Q of the ring resonator (called the unloaded Q) is a measure of the losses only in the resonator. The unloaded Q is obtained by separating the external losses in the feed line and due to coupling. The loaded Q and the unloaded Q are related through the reflection coefficients at and far from resonance.[16] The derivation for the relationship between the loaded Q and the unloaded Q is described by Aitken.[16] A computer program was written to compute the unloaded Q values from the measured loaded Q and the magnitude of reflection coefficients at and far from resonance. The determination of whether the resonator was overcoupled or undercoupled was made from the Smith chart and also the phase response of the resonator. Typically, the ring resonators were overcoupled. Measurements for the superconducting resonator were performed at the fundamental resonance frequency of 12 GHz and an input power level of -30 dBm.

Unloaded Q versus temperature characteristics for two ring resonators is shown in Fig. 6. Curve A is the data for the high-T_c thin-film ring resonator with a superconducting ground plane. For comparison, data for the gold resonator with a gold ground plane is shown by curve B. The unloaded Q of the ring resonator with superconducting ground plane is approximately four times higher than the gold resonator at 65 K. In addition, the unloaded Q of the superconducting ring resonator shows an increasing trend in Q with decreasing temperature, whereas the superconducting ring resonators with gold ground plane show a saturation of Q at low temperatures due to the dominance of ground plane conductor losses.

The superconducting ring resonators offer an indirect method for measuring the surface resistance R_s of the superconducting thin films. This microwave surface resistance is the fundamental quantity responsible for the conductor losses at high frequencies. The R_s of sputtered thin films were obtained from ring resonator quality factor Q measurements. By separating the conductor and dielectric losses, the surface resistance of the TlCaBaCuO thin films was calculated using the standard microstrip loss equations described by Pucel, Masse, and Hartwig.[17] The R_s at 12 GHz and 77 K was determined to be typically between 1.5 and 2.75 mΩ, almost an order of magnitude lower than R_s of Cu at the same temperature and frequency.

The swept frequency reflection measurements performed at several temperatures are also used in determining the penetration depth of the TlCaBaCuO superconducting thin films. The resonance frequency is the frequency at which the magnitude of the reflection coefficient is at the minimum. The resonance frequency was measured at each temperature for ring resonators. A typical measured resonance frequency shift with respect to temperature for a superconducting ring resonator with an approximately 1-μm-thick gold ground plane is shown in Fig. 7. The shift in resonance frequency with temperature is mainly due to the temperature dependence of the penetration depth of the superconductor. Thus, the resonance frequency shift is an indirect method of determining the penetration depth. From the figure, the change in resonance frequency below 70 K is almost negligible. The superconducting resonators with a 0.3-μm-thick superconducting ground plane showed a slightly higher dependence of resonance frequency with temperature due to the temperature dependence of penetration depths of the top and the ground plane superconductors. A detailed analysis of this figure to determine the penetration depth of the superconducting thin films is given in the following section.

IV. ANALYSIS AND DISCUSSIONS

The data from the zero-field current density J_c measurements shown in Fig. 4 were analyzed to investigate the

dependence of J_c with the temperature ratio T/T_c. The slope of the $\log J_c$ vs $\log(1-T/T_c)$ characteristics is an indication of the type of the superconductor. The slope of the line obtained from our measurements was approximately 1.5 for temperatures between 50 and 80 K. The $(1-T/T_c)^{3/2}$ dependence of J_c is consistent with earlier reports in high-T_c thin films.[18] This indicates that the thin films may contain grain boundaries that are either insulating or behave like a normal metal, or the thin films may be polycrystalline in nature. The presence of grain boundaries and weak flux pinning in TlCaBaCuO thin films may be the main reasons for the lower J_c in TlCaBaCuO thin films compared to epitaxial *in situ* grown YBaCuO thin films. However, among the polycrystalline high-T_c thin films, TlCaBaCuO thin films have shown superior electrical properties and hence are very attractive for electronic applications.

The penetration depth of TlCaBaCuO thin films can be determined from the resonance frequency versus temperature measurements, by comparing the experimental data shown in Fig. 7 with theoretical calculations. The resonance frequency shift in the ring resonators is assumed to be due to the change in penetration depth with temperature. Neglecting the effects due to the substrate contraction at lower temperatures, the penetration depth was extracted from the resonance frequency shift as discussed below.

The phase velocity of a superconducting microstrip transmission line with a superconducting ground plane is given by[19]

$$v_{ph}=c/\sqrt{\epsilon_{eff}}[1+2\lambda/h\coth(t/\lambda)]^{-0.5}, \tag{1}$$

where c is the velocity of light, ϵ_{eff} is the effective dielectric constant, h is the substrate thickness, t is the thickness of the microstrip, and λ is the penetration depth of the superconducting microstrip. The penetration depth is temperature dependent based on the Gorter–Casimir relationship,[20] i.e.,

$$\lambda(T)=\lambda(0)[1-(T/T_c)^4]^{-0.5}, \tag{2}$$

for temperature T less than T_c. $\lambda(0)$ is the penetration depth at $t=0$ K. The resonance frequency of the ring resonator is given by the equation

$$f=nv_{ph}/(2L), \tag{3}$$

where f is in GHz, L is the mean circumference of the ring in mm, and n is the integer order of resonance. From the temperature dependence of resonance frequency measurements and the above equations, the best value of $\lambda(0)$ was determined to be 6890 Å. The typical value ranges between 7000 and 8000 Å. This is an approximate estimate for the penetration depth along the c axis in the TlCaBaCuO thin films. Since the thin films are only 0.3–0.4 μm thick, the penetration depth depends upon the properties of the superconductor through the entire film. This may be a reason for the high penetration depth. Also, the patterned thin films have rough edges, and hence the penetration depth obtained using the above technique is an averaged value over the whole film area.

The surface resistance of the TlCaBaCuO superconducting thin films determined from the ring resonator Q measurements was compared with the theoretical surface resistance versus temperature characteristics for a given penetration depth. A theoretical model based on the phenomenological loss equivalence method (PEM) approximation[21,22] was employed to determine the theoretical variation of conductor losses and the surface resistance with temperature for the cases of superconducting microstrip/gold ground plane, and superconducting microstrip/superconducting ground plane. Both these cases were compared to the attenuation constant of a gold microstrip on $LaAlO_3$ substrate.

The attenuation constant for a superconducting microstrip is calculated from the formula[22]

$$\alpha=(T/T_c)^4/[1-(T/T_c)^4]^{3/2}(G_1/4)(\sigma_n/Z)\times w^2\mu^2[\lambda(0)^3]\coth(X)+X\operatorname{cosec}^2(X)(Np/m), \tag{4}$$

where

$$X=A[G_1/\lambda(0)][1-(T/T_c)^4]^{1/2}.$$

G_1 is the geometric factor given by the equation

$$G_1=1/(\pi h)\{1-[W_e/(4h)]^2\}[1/2+h/W_e+h/(\pi W_e)\ln(2h/t)], \tag{5}$$

where W_e is the effective width of the microstrip, A is the area of cross section of the microstrip, T is the measurement temperature below T_c, and $\lambda(0)$ the penetration depth at 0 K of the superconductor.

The parameters assumed for the calculations are the relative dielectric constant ϵ_r of $LaAlO_3$ of 24.5, the loss tangent ($\tan\delta$) of $LaAlO_3$ of 8.3×10^{-5} below 100 K, the substrate thickness h of 10 mil, the width of the microstrip W of 142 μm, corresponding to a characteristic impedance of 41 Ω at 12 GHz, the thickness of the superconducting microstrip t of 0.3 μm, the ground plane thickness of 1 μm for a gold ground plane and 0.3 μm for a superconducting ground plane, the zero resistance T_c of the TlCaBaCuO thin films of 100 K, and the normal conductivity at T_c (σ_n) of 1.5×10^6 S/m.

The ground plane conductor losses can be calculated by the same method, using the geometric factor G_2 instead of G_1 in Eq. (4),

$$G_2=1/(2\pi h)[1-(W_e/4h)^2]. \tag{6}$$

Figure 8 shows temperature variation of the attenuation due to conductor losses for a gold microstrip (curve A), a superconducting microstrip with a gold ground plane (curve B), and a superconducting microstrip with a superconducting ground plane (curve C) as determined using Eqs. (4)–(6). The upper diagram is for $\lambda(0)$ of 6000 Å, and the lower diagram is for $\lambda(0)$ of 7000 Å. Figure 8 shows the lower attenuation for the microstrip with superconducting ground plane (curve C) compared to the one with gold ground plane (curve B) below 77 K.

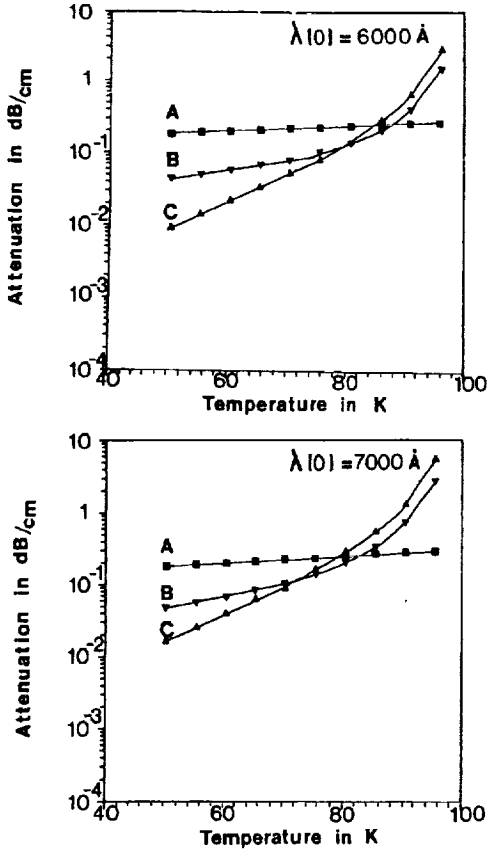

FIG. 8. Theoretical temperature variation of attenuation due to conductor losses for a gold microstrip (1-μm-thick gold for both sides: curve A), a superconducting microstrip (0.3 μm) with a gold ground plane (1 μm) in curve B, and a superconducting microstrip (0.3 μm) with a superconducting ground plane (0.3 μm) in curve C. The penetration depth at 0 K was assumed to be 6000 Å for the upper diagram and 7000 Å for the lower diagram.

The surface resistance of the superconducting thin film is obtained from the equation

$$R_s = 2Z_0\alpha/G_1, \tag{7}$$

where Z_0 is the characteristic impedance of the microstrip. The theoretical temperature variation of surface resistance of the superconducting microstrip with a superconducting ground plane determined using Eq. (7) is shown in Fig. 9, for $\lambda(0)$ of 6000 Å (curve C) and 7000 Å (curve B). For comparison, the surface resistance of a 1-μm-thick gold microstrip (curve A) on a $LaAlO_3$ substrate is plotted for the same microstrip geometry. The R_s calculated from the measured Q values of an all-superconducting ring resonator on a $LaAlO_3$ substrate (curve D) is also plotted in Fig. 9. The R_s obtained from the ring resonator Q measurements (curve D) deviates from the theoretical temperature dependence as seen in the figure. Since the TlCaBaCuO thin films do react with the $LaAlO_3$ substrate, it is possible that the region of interaction contributes to additional losses.

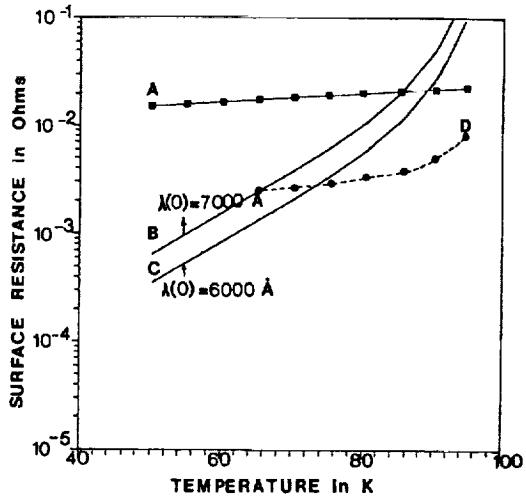

FIG. 9. Theoretical temperature variation of surface resistance for the all-superconducting ring resonator, for penetration depths at 0 K of 6000 (curve C) and 7000 Å (curve B). The surface resistance calculated from the measured Q values of the resonator is also shown in curve D. For comparison, the surface resistance of a gold microstrip is plotted in curve A.

V. SUMMARY

TlCaBaCuO superconducting thin films were fabricated on $LaAlO_3$ substrates by rf magnetron sputter deposition in a pure argon plasma and by using postannealing techniques. A reproducible fabrication process has been established for TlCaBaCuO thin films on $LaAlO_3$ substrates for high-T_c and high-J_c characteristics. The TlCaBaCuO thin films were patterned into four-probe test devices using standard microelectronic lithography and wet etching techniques. Low-resistance gold contacts on TlCaBaCuO thin films were obtained by annealing at 600 °C in an oxygen flow of 1 l/min followed by a slow furnace cooling for about 30 min. The critical current density measurements were performed using dc and pulsed current techniques under the electric-field criterion of 1 μV/mm. The zero-resistance T_c between 97 and 100 K are routinely obtained in patterned TlCaBaCuO thin films. Zero-field current density J_c as high as 5×10^5 A/cm^2 were obtained in four-probe test devices. The specific contact resistivity measured when the sample is superconducting ranges from 3.65×10^{-5} Ω cm^2 at 90 K, to 10^{-10} Ω cm^2 below 77 K.

The microwave properties of TlCaBaCuO thin films were investigated by designing, fabricating, and characterizing a microstrip ring resonator. The resonator was designed for a fundamental resonance frequency of 12 GHz, and for fabrication on 10-mil-thick $LaAlO_3$ substrates. Ring resonators with a gold ground plane of 1 μm thickness and a TlCaBaCuO superconducting ground plane of 0.3 μm thickness were fabricated and characterized at cryogenic temperatures. The unloaded Q for the superconducting resonators were above 1500 at 65 K, compared to 370 for a gold resonator. The surface resistance of the TlCaBaCuO thin films obtained by separating conductor losses from the Q measurements is typically between 1.5

and 2.75 m-Ω at 12 GHz and 77 K, almost an order lower than Cu and Au at the same temperature and frequency. The penetration depth at 0 K was calculated from the resonance frequency shift with temperature measurements. The typical values for the penetration depth at 0 K are approximately between 7000 and 8000 Å.

The conductor losses in the superconducting microstrips with superconducting ground plane were compared to the ones with gold ground plane using a theoretical model called the phenomenological loss equivalence method (PEM). This model predicted lower conductor losses for the microstrip with a superconducting ground plane, below 77 K. A theoretical temperature variation of the surface resistance R_s for different penetration depths was obtained for the all-superconducting microstrip (with superconducting ground plane). The R_s obtained from the Q measurements in the ring resonators deviates from the theoretical temperature dependence. This is possibly because of additional losses introduced in the devices due to interaction between the TlCaBaCuO thin films and the $LaAlO_3$ substrates. Nevertheless, the polycrystalline TlCaBaCuO thin films have almost an order-of-magnitude lower surface resistance compared to gold at 80 K. The design of the ring resonator was not optimized for the highest Q, but the results of our investigations show that TlCaBaCuO ring resonator devices fabricated with a superconducting ground plane do show higher Q compared to a gold resonator below 90 K, proving their usefulness for all-superconducting microwave circuit applications.

ACKNOWLEDGMENTS

The authors thank Dr. Regis Leonard for his continued support and encouragement. The authors thank Dr. Sam Alterovitz, Dr. Mark Stan, and Dr. John Pouch for useful discussions, and also thank Professor Punit Boolchand for his useful suggestions and discussions. This research was supported by NASA Lewis Research Center.

[1] J. G. Bednorz and K. A. Muller, Z. Phys. B **64**, 189 (1986).
[2] M. K. Wu, J. R. Ashburn, C. J. Torng, P. H. Hor, R. L. Meng, L. Gao, Z. J. Huang, Y. Q. Wang, and C. W. Chu, Phys. Rev. Lett. **58**, 908 (1987).
[3] H. Maeda, Y. Tanaka, M. Fukitomi, and T. Asano, Jpn. J. Appl. Phys. **27**, L209 (1988).
[4] Z. Z. Sheng and A. M. Hermann, Nature **332**, 138 (1988).
[5] L. D. Chang, M. J. Moskowitz, R. B. Hammond, M. M. Eddy, W. L. Olson, D. D. Casavant, E. J. Smith, M. Robinson, L. Drabeck and G. Gruner, Appl. Phys. Lett. **55**, 1357 (1989).
[6] L. C. Bourne, R. B. Hammond, McD. Robinson, M. M. Eddy, W. L. Olson, and T. W. James, Appl. Phys. Lett. **56**, 2333 (1990).
[7] R. B. Hammond, G. V. Negrete, M. S. Schmidt, M. J. Moskowitz, M. M. Eddy, D. D. Strother, and D. L. Skoglund, in Proceedings of the IEEE MTT Symposium, June 1990.
[8] C. Wilker, Z. Y. Shen, P. Pang, D. W. Face, W. L. Holstein, A. L. Mathews, and D. B. Laubacher, IEEE Microwave Theory Tech. **MTT-39**, 1462 (1991).
[9] S. S. P. Parkin, V. Y. Lee, E. M. Engler, A. I. Nazzal, T. C. Huang, G. Gorman, R. Savoy, and R. Beyers, Phys. Rev. Lett. **60**, 2539 (1988).
[10] W. Y. Lee, V. Y. Lee, J. Salem, T. C. Huang, R. Savoy, D. C. Bullock, and S. S. P. Parkin, Appl. Phys. Lett. **53**, 329 (1988).
[11] D. S. Ginley, J. F. Kwak, E. L. Venturini, B. Morosin, and R. J. Baughman, Physica C **160**, 42 (1989).
[12] G. Subramanyam, F. Radpour, V. J. Kapoor, and G. H. Lemon, J. Appl. Phys. **68**, 1157 (1990).
[13] G. Subramanyam, F. Radpour, and V. J. Kapoor, Appl. Phys. Lett. **56**, 799 (1990).
[14] G. Subramanyam, V. J. Kapoor, and G. H. Lemon, Bull. Am. Phys. Soc. **36**, 519 (1991).
[15] C. M. Chorey, K. S. Kong, K. B. Bhasin, J. D. Warner, and T. Itoh, IEEE Trans. Microwave Theory Tech. **39**, 1480 (1991).
[16] J. Aitken, Proc. Inst. Electr. Eng. **123**, 855 (1976).
[17] R. A. Pucel, D. J. Masse, and C. P. Hartwig, IEEE Trans. Microwave Theory Tech. **MTT-16**, 342 (1968); **16**, 1064 (1968).
[18] J. F. Kwak, D. S. Ginley, E. L. Venturini, B. Morosin, R. J. Baughman, J. C. Barbour, and M. O. Eatough, in *Studies of High Temperature Superconductors*, edited by A. Narlikar (Nova Science, New York, 1991), Vol. 7, pp. 45–73.
[19] R. L. Kautz, J. Appl. Phys. **49**, 308 (1978).
[20] T. Van Duzer and C. W. Turner, *Principles of Superconductive Devices and Circuits* (Elsevier/North-Holland, New York, 1981), Chap. 3, pp. 92–138.
[21] H. -Y. Lee and T. Itoh, IEEE Trans. Microwave Theory Tech. **MTT-37**, 1904 (1989).
[22] O. R. Baiocchi, K. -S. Kong, H. Ling, and T. Itoh, IEEE Microwave Guided Wave Lett. **MGWL-1**, 2 (1991).